High Performance Computing Simulations for a Subsonic Projectile with Jet Interactions

Jubaraj Sahu
U.S. Army Research Laboratory
Aberdeen Proving Ground, MD 21005

Keywords: HPC computing, numerical simulations, subsonic flow, jet interactions, computational fluid dynamics, projectile aerodynamics

Abstract

This paper describes a computational study undertaken to consider the aerodynamic effect of small tiny jets as a means to provide the control authority needed to maneuver a projectile at low subsonic speeds. Scalable Navier-Stokes computational technique has been used to obtain numerical solutions for the unsteady jet-interaction flow field for a projectile at subsonic speeds. Computed results have been obtained at a low subsonic speed at zero degree angle of attack. Qualitative flow field features show the interaction of the time-dependent jet with the free stream flow. Numerical results show the effect of the jet on the flow field and surface pressures and, hence, on the aerodynamic coefficients. Unsteady jet results have been obtained for a two-dimensional jet flow and compared with experimental data for validation. The same unsteady jet modeling technique has been applied to a subsonic projectile. These numerical results are being assessed to determine if small synthetic jets can be used to provide the control authority needed for maneuvering munitions to hit the targets with precision.

INTRODUCTION

The prediction of aerodynamic coefficients for projectile configurations is essential in assessing the performance of new designs. Accurate determination of aerodynamics is critical to the low-cost development of new advanced guided projectiles, rockets, missiles, and smart munitions. Fins, canards, and jets can be used to provide control for maneuvering projectiles and missiles. The flow fields associated with these control mechanisms for the Army weapons are complex involving three-dimensional (3-D) shock-boundary layer interactions, jet-interaction with the free stream flow, and highly viscous dominated separated flow regions [1–3]. The jet interference extends over significant portions of the projectile and must be modeled correctly. For missiles, jet thrusters have been studied over a number of years to provide high-speed aerodynamic control. These thrusters interact with the surrounding flow field and the resulting jet interaction flow field again is complex. Recently, several studies have shown that small tiny synthetic unsteady jets can significantly alter the flow field and pressure distributions for airfoils and cylinders. The present analysis involves these tiny jets for projectile aerodynamic control. The emphasis in the present research is to provide insight into the interaction of these unsteady jets with the free stream flow and to determine the feasibility of these jets for aerodynamic control of a subsonic projectile. Both computational and experimental data for these jet interactions are very limited. Simple theories cannot predict the complex flow fields associated with the jet interaction, and experimental tests are very expensive. To help reduce experimental costs, computational fluid dynamics (CFD) is being used to predict these complex flows and provide detailed pressure, and force and moment data. The advanced CFD capability used here solves the Navier-Stokes equations [4] and incorporates unsteady boundary conditions for simulation of the synthetic jets. Also, a hybrid Reynolds-Averaged Navier-Stokes (RANS)/ Large Eddy Simulation (LES) turbulence model was used for accurate numerical prediction of unsteady jet flows. Numerical flow field computations have been made for both steady and unsteady jets for a projectile configuration at a low subsonic speed. The following sections describe the numerical procedure and the computed results obtained.

NUMERICAL SOLUTION TECHNIQUE

The complete set of 3-D time-dependent Navier-Stokes equations is solved in a time-accurate manner for simulations of unsteady jets.

A commercially available code, CFD++ [5–7], is used for the time-accurate unsteady CFD simulations. The basic numerical framework in the code contains unified-grid, unified-physics, and unified-computing features. The user is referred to these references for details of the basic numerical framework. Here, only a brief synopsis of this framework and methodology is given.

The 3-D time-dependent Reynolds-averaged Navier-Stokes (RANS) equations are solved using the finite volume method:

$$\frac{\partial}{\partial t}\int_V \mathbf{W}\,dV + \oint\left[\mathbf{F}-\mathbf{G}\right]\cdot dA = \int_V \mathbf{H}\,dV$$

(1)

where **W** is the vector of conservative variables, **F** and **G** are the inviscid and viscous flux vectors, respectively, **H** is the vector of source terms, V is the cell volume, and A is the surface area of the cell face.

The numerical framework of CFD++ is based on the following general elements: (1) unsteady compressible and incompressible Navier-Stokes equations with turbulence modeling [unified-physics], (2) unification of Cartesian, structured curvilinear, and unstructured grids, including hybrids [unified-grid], (3) unification of treatment of various cell shapes including 3-D hexahedral, tetrahedral and triangular prism cells, two-dimensional (2-D) quadrilateral and triangular cells and one-dimensional (1-D) linear elements [unified-grid], (4) treatment of multiblock patched aligned (nodally connected), patched-nonaligned and overset grids [unified-grid], (5) Total Variation Diminishing discretization based on a new multi-dimensional interpolation framework, (6) Riemann solvers providing proper signal propagation physics, including versions for preconditioned forms of the governing equations, (7) consistent and accurate discretization of viscous terms using the same multidimensional polynomial framework, (8) pointwise turbulence models not requiring knowledge of distance to walls, (9) versatile boundary condition implementation including a rich variety of integrated boundary condition types for the various sets of equations, (10) implementation on massively parallel computers based on the distributed-memory message-passing model using native message-passing libraries or MPI, PVM, etc. [unified-computing].

The code has brought together several ideas on convergence acceleration to yield a fast methodology for all flow regimes. The approach can be labeled as a "preconditioned-implicit-relaxation" scheme. It combines three basic ideas: (1) implicit local time-stepping, (2) relaxation, and (3) preconditioning. Preconditioning the equations ideally equalizes the eigenvalues of the inviscid flux Jacobians and removes the stiffness arising from large discrepancies between the flow and sound velocities at low speeds. Use of an implicit scheme circumvents the stringent stability limits suffered by their explicit counterparts, and successive relaxation allows update of cells as information becomes available and thus aids convergence. These features of the code have been extremely useful in the present numerical simulations at very low subsonic speeds.

The code also uses a multidimensional interpolation that more accurately represents local behavior of flow-dependent variables. Second-order discretization was used for the flow variables and the turbulent viscosity equation. The turbulence closure is based on topology-parameter-free formulations. Two-equation and higher order hybrid RANS/LES turbulence models were used for the computation of turbulent flows. These models are ideally suited to unstructured book-keeping and massively parallel processing due to their independence from constraints related to the placement of boundaries and/or zonal interfaces.

RESULTS

For computational validation purposes, CFD was first used to compute the flow for an isolated 2-D jet case shown in Figure 1. This figure shows a schematic diagram along with a flow picture obtained from the experiment. Here the jet width is 0.5 mm and the peak jet velocity is 20 m/s. The jet actuator operates at a frequency of 1000 Hz [8]. In the numerical computations, unsteady jet boundary conditions were applied at the jet exit and the actual cavity was not modeled. A sinusoidal variation was used for the jet exit velocity with a peak amplitude of 20 m/s. Computed velocity and vorticity contours are shown in Figure 2.

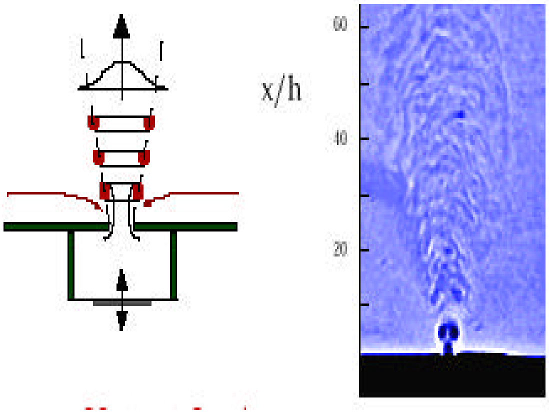

Figure 1. Schematic of a 2-D unsteady jet in experiment.

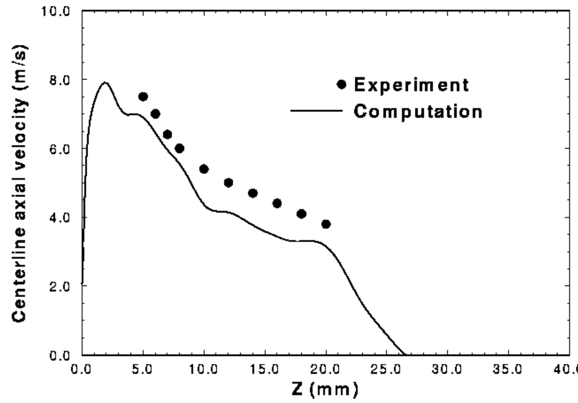

Figure 3. Variation of time-averaged centerline jet velocity with distance from the wall.

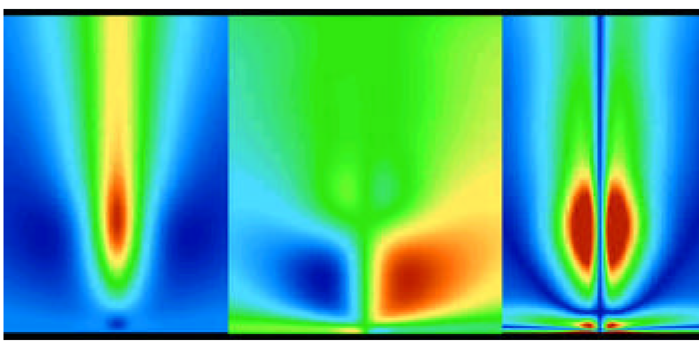

Figure 2. Contours of velocity components (u, v) and vorticity (from left to right).

The time-averaged jet centerline velocity over many cycles is compared with available experimental data in Figure 3, and is found to be in reasonable agreement. As shown both in the experiment and the computations, the time-averaged centerline velocity is decreased with increasing distance away from the jet exit (increasing z in the x-axis in Figure 3). CFD technique described earlier was then applied to compute the flow over a projectile.

The subsonic projectile is a 1.8-caliber ogive-cylinder configuration (see Figure 4). Here, the primary interest is in the development and application of CFD techniques for accurate simulation of projectile flow field in the presence of unsteady jets. The first step here is to obtain the steady state results for the same projectile without the jet. Converged jet-off steady state solution was then used as the starting condition for the computation of time-accurate unsteady flow field for the projectile with synthetic jets. Computations were also performed for the steady jet cases. The jet locations on the projectile are shown in Figure 5. The jet conditions were specified at the exit of the jet for both steady (fixed jet velocity) and unsteady (sinusoidal variation in jet velocity) jets. The jet conditions specified include the jet pressure, density and velocity components. The flow field inside of the tiny jet cavity is not computed. For the unsteady jet case, time-dependent jet boundary conditions are applied at the jet exit. Numerical computations have been made for these jet cases at a Mach number, M = 0.11 and at an angle of attack, a = 0^o. The jet width was 0.32 mm, the jet slot half-angle was 18^o, and the peak jet velocity used was 31 m/s operating at a frequency of 1000 Hz.

A computational grid expanded near the vicinity of the projectile is shown in Figure 6. Grid points are clustered near the jet as well as the boundary layer regions to capture the high gradients flow regions. The computational grid has 211 points in the streamwise direction, 241 in the circumferential direction, and 80 in the normal direction. The unsteady simulation took thousands of hours of CPU time on a Silicon Graphics Origin computer running with 24 processors.

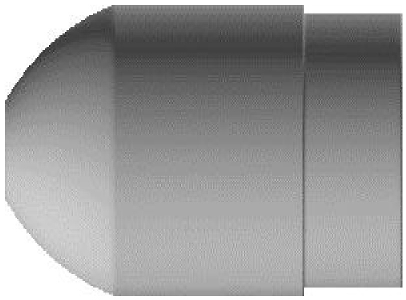

Figure 4. Projectile model geometry.

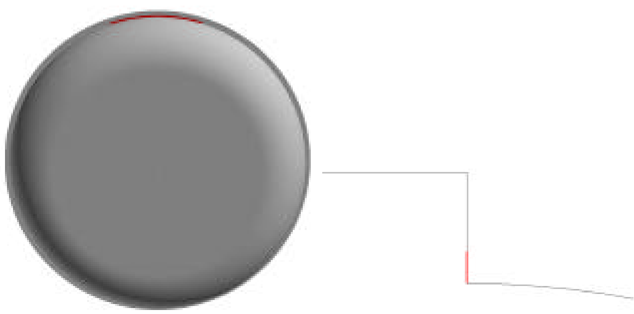

Figure 5. Aft-end geometry showing the jet location.

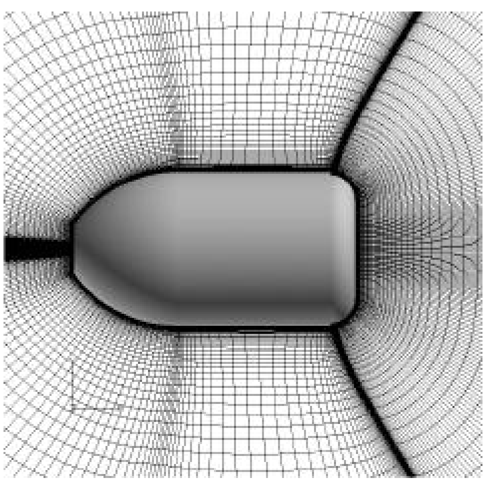

Figure 6. Computational grid near the projectile.

Computed pressure contours for the jet-off case at M = 0.11 and $\alpha = 0°$ are shown in Figure 7. This figure shows a high pressure region near the nose and low pressures in the near wake. Computed velocity vectors for this case are shown in Figure 8. The recirculatory flow regions in the wake and near the step upstream of the base are clearly evident. As seen in this figure, the flow field in the base region is fairly symmetric. The flow field results for the case with the synthetic jet-on are shown in Figures 9 and 10. These figures show the qualitative flow features near the jet as well as the base region of the projectile. Figure 9 shows the velocity vectors at a given instant in time. It clearly shows the flow in the base region to be asymmetric due to the interaction of the unsteady jet. The shear layer from the free stream flow resulting from the step corner upstream of the base interacts with the unsteady jet and breaks down just a short distance downstream of the jet. The jet has a strong effect on the pressure distribution both upstream and downstream of the jet location (see Figure 10). The pressure field both upstream and downstream of the jet is clearly affected by the jet flow depending on whether the flow is going into or out of the cavity. The computed flow field again is asymmetric. Figure 10 also shows regions of alternating low and high pressure just downstream of the jet indicating vorticity being shed from the jet exit into the base region flow.

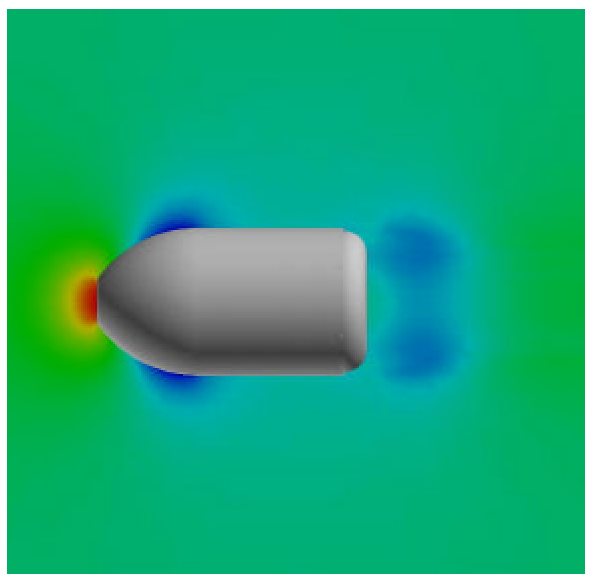

Figure 7. Computed pressures, jet-off, M = 0.11, $\alpha = 0°$.

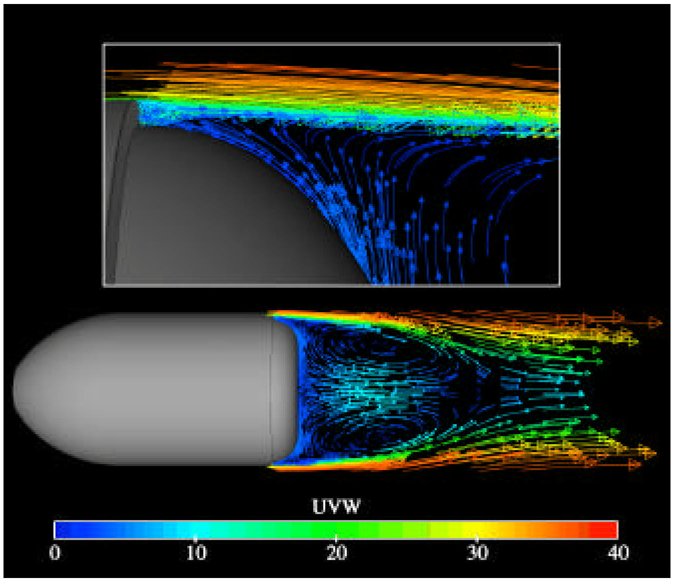

Figure 8. Computed velocity vectors, jet-off, M = 0.11,α = 0°.

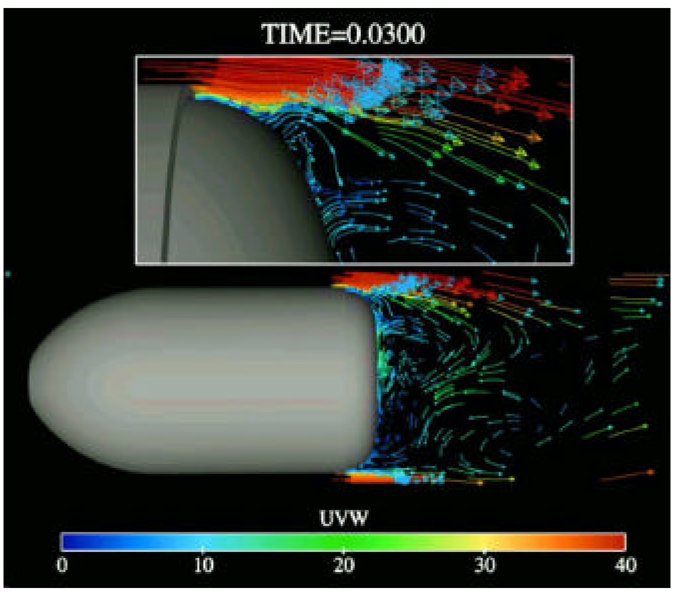

Figure 9. Computed velocity vectors, jet-on, M = 0.11, α = 0°.

The resulting surface pressures from the unsteady flow fields are integrated to obtain the aerodynamic forces and moments. The computed axial force, the normal force, and the pitching moment are shown in

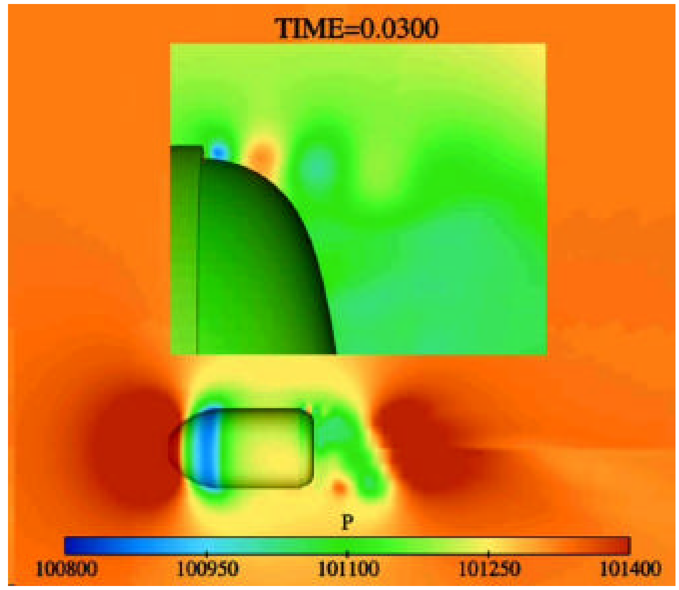

Figure 10. Computed pressures, jet-on, M = 0.11, α = 0°.

Figures 11, 12, and 13 as a function of time, respectively. These computed results clearly indicate the unsteady nature of the flow field. All these forces and moment are found to change as a function of time. Changes in the drag force and pitching moment are smaller than that of the lift force over the first 20 ms. The unsteady interactions of the synthetic jet and the wake flow of the projectile usually requires hundreds of cycles of the jet operations before a truly unsteady periodic flow is established. Currently, computations have been extended to achieve that. Also, large amount of CFD datasets are saved at regular intervals to analyze the fully unsteady periodic nature of the flow field requiring huge computer resources both in terms of storage and flow visualization. The computed results obtained thus far are being analyzed to determine the feasibility of the synthetic jets to provide control authority. The next challenge is to utilize the current methods to the same projectile but with spin and yaw. Future efforts will require large unsteady numerical computations to optimize the number and locations of the synthetic jets. It is anticipated that multiple jets may be required to provide the control authority needed for maneuvering a subsonic projectile and will require use of a coupled CFD and controls technique to jet divert control authority.

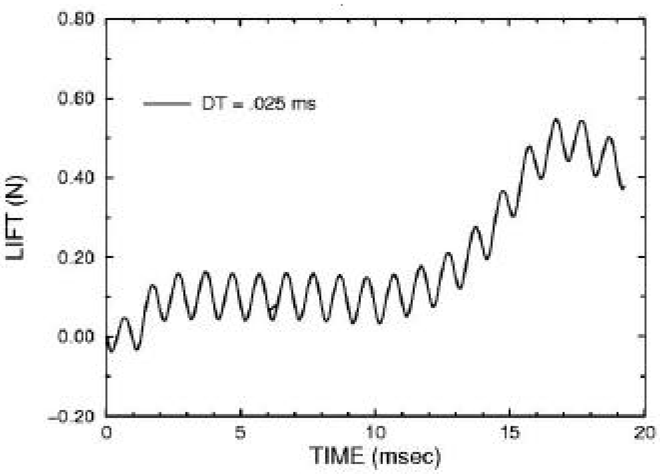

Figure 11. Computed lift force, M = 0.11, $\alpha = 0°$.

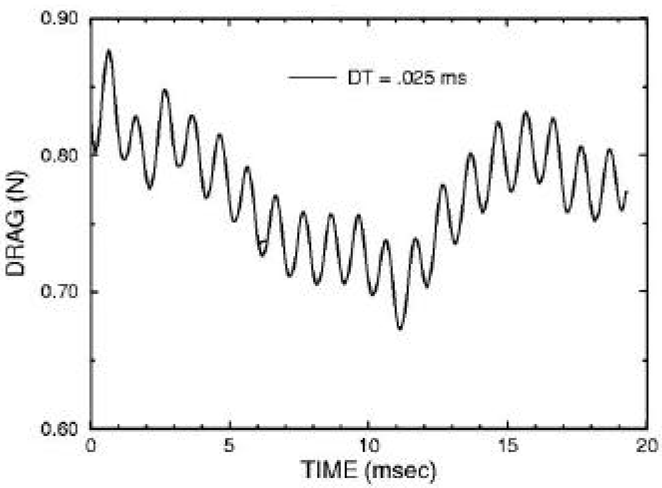

Figure 12. Computed drag force, M = 0.11, $\alpha = 0°$.

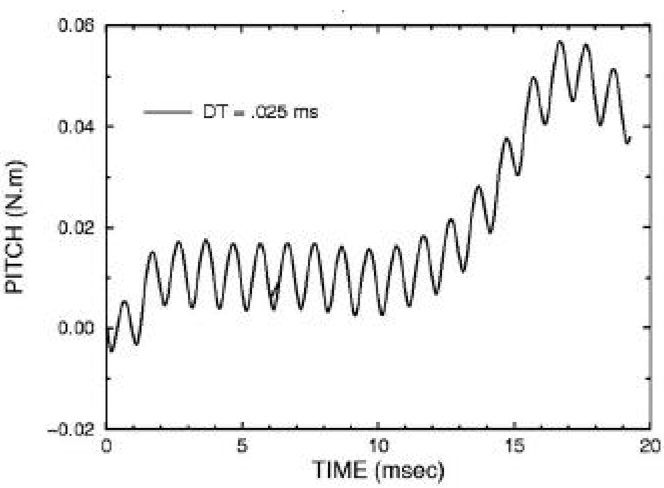

Figure 13. Computed pitching moment, M = 0.11, $\alpha = 0°$.

CONCLUDING REMARKS

This paper describes a computational study undertaken to determine the aerodynamic effect of tiny synthetic jets as a means to provide the control authority needed to maneuver a projectile at low subsonic speeds. Computed results have been obtained at a low subsonic speed and zero degree angle of attack for a subsonic projectile using Navier-Stokes computational technique and advanced turbulence models. Qualitative flow field features show the interaction of tiny synthetic jet with the free stream flow and the large extent of influence both upstream and downstream of the jet. The unsteady jet results obtained for a 2-D jet are compared with the data and are found to be in reasonable agreement. The unsteady jet in the case of the subsonic projectile is shown to substantially alter the flow field both near the jet and the base region that in turn affects the forces and moments even at zero degree angle of attack. The results show the potential of CFD to provide insight into the jet interaction flow fields and provide guidance as to the locations and sizes of the jets to generate the maximum control authority for maneuvering smart munitions. Current and future efforts are directed towards the addition of spin and yaw to these large unsteady synthetic jet computations for application to a spinning projectile. Future efforts will also include the optimization of the number and location of the synthetic jets as well as coupling of CFD and controls to accurately determine the control authority needed for maneuvering a subsonic spinning projectile.

ACKNOWLEDGMENTS

This work was accomplished as part of a Defense Advanced Research Projects Agency (DARPA) sponsored and jointly funded research project by the U.S. Army Research Laboratory (ARL) on Micro Adaptive Flow Control. The author wishes to thank the members of the project team consisting of Georgia Tech Research Institute (GTRI), Metacomp Technologies, and for their help. The scientific visualization work of R. Angelini of ARL and the computational support of the ARL Major Shared Resource Center are greatly appreciated.

REFERENCES

1. Sahu, J., K. R. Heavey, and E. N. Ferry, "Computational Fluid Dynamics for Multiple Projectile Configurations." Proceedings of the 3rd Overset Composite Grid and Solution Technology Symposium, Los Alamos, NM, October 1996.

2. Sahu, J., K. R. Heavey, and C. J. Nietubicz, "Time-Dependent Navier-Stokes Computations for Submunitions in Relative Motion." Proceedings of the 6th International Symposium on Computational Fluid Dynamics, Lake Tahoe, NV, September 1995.

3. Meakin, R. L., "Computations of the Unsteady Flow About a Generic Wing/Pylon/Finned-Store Configuration." AIAA 92-4568-CP, August 1992.

4. Pulliam, T. H., and J. L. Steger, "On Implicit Finite-Difference Simulations of Three- Dimensional Flow." *AIAA Journal*, vol. 18, no. 2, pp. 159–167, February 1982.

5. Peroomian, O., S. Chakravarthy, and U. Goldberg, "A 'Grid-Transparent' Methodology for CFD." AIAA Paper 97-07245, 1997.

6. Peroomian, O., S. Chakravarthy, S. Palaniswamy, and U. Goldberg, "Convergence Acceleration for Unified-Grid Formulation Using Preconditioned Implicit Relaxation." AIAA Paper 98-0116, 1998.

7. Goldberg, U. C., O. Peroomian, and S. Chakravarthy, "A Wall-Distance-Free K-E Model With Enhanced Near-Wall Treatment." *ASME Journal of Fluids Engineering*, Vol. 120, pp. 457-462, 1998.

8. Smith B. L., and A. Glezer, "The Formation and Evolution of Synthetic Jets." *Journal of Physics of Fluids*, vol. 10, no. 9, September 1998.